



UPPSALA  
UNIVERSITET

# **Role of mast cells in an in-vivo model of COPD-associated inflammation**

**Erik Danielsson**

---

Master Degree Project in Infection Biology, 30.0 credits. Spring  
2020

Department of Medical Biochemistry and Microbiology (IMBIM)

Lab Supervisor: Eduardo Cárdenas, PhD

Supervisor: Jenny Hallgren Martinsson, PhD

## Table of Contents

<b>Abstract:</b> .....	<b>4</b>
<b>Popular science summary:</b> .....	<b>5</b>
<b>§1: Introduction</b> .....	<b>6</b>
§1.1: Chronic Obstructive Pulmonary Disease (COPD) .....	6
§1.2: Mouse models of COPD .....	9
§1.3: Mast cells .....	10
<b>Aim</b> .....	<b>13</b>
<b>§2: Methods</b> .....	<b>14</b>
<b>Ethics</b> .....	<b>14</b>
§2.1: Mice .....	14
§2.2: Genotyping of Cpa3 <sup>Cre/+</sup> mice .....	14
§2.3: LPS/elastase protocol to induce COPD-like inflammation .....	15
§2.4: Bronchoalveolar lavage fluid .....	16
§2.5: Lung digestion .....	16
§2.6: Flow cytometry .....	16
§2.7: Statistics .....	18
<b>§3: Results</b> .....	<b>19</b>
§3.1 Validation of COPD model .....	19
§3.2 Mast cells appear not to be required for COPD-associated lung inflammation. ....	23
§3.3 A single intranasal dose of LPS induces an increase in total BALF cells, neutrophils, and CD4+ T-cells. ....	24
§3.4 A single dose of intranasal elastase did not induce lung inflammation .....	27
<b>§4: Discussion</b> .....	<b>28</b>
<b>Acknowledgements</b> .....	<b>30</b>
<b>References</b> .....	<b>31</b>

**Abbreviations:**

<b>BALF</b>	Bronchoalveolar lavage fluid
<b>COPD</b>	Chronic obstructive pulmonary disease
<b>Cpa3<sup>Cre/+</sup> mice</b>	Strain of mast cell-deficient mice
<b>i.n.</b>	Intranasal
<b>Lin</b>	Lineage
<b>LPS</b>	Lipopolysaccharide
<b>MC</b>	Mast cell
<b>MCD</b>	Mast cell deficient
<b>MCp</b>	Mast cell progenitor
<b>mMCP</b>	Mouse mast cell protease
<b>PBS</b>	Phosphate buffered saline
<b>WT</b>	Wild-type

**Abstract:**

Chronic Obstructive Pulmonary Disease (COPD) is a common lung disease characterized by progressive and irreversible airway obstruction, and mainly caused by a chronic exposure to lung irritants. As of 2010, 384 million people suffered from COPD worldwide. It is widely accepted that a chronic inflammatory response is integral to COPD pathogenesis and linked to disease progression. The cellular mediators and molecular mechanisms of COPD-associated inflammation are not completely understood and are difficult to emulate in animal models, which hinders the development of better treatments. In this study, experimental COPD and its associated inflammation were induced in mice using a 4-week protocol involving intranasal administration of LPS and elastase. Model validation on wild-type mice yielded COPD-like disease judging from flow cytometric analyses with and pulmonary function testing. After 4 weeks of exposure to LPS and elastase, mice developed classic aspects of COPD such an increase in lung-infiltrating cells, (e.g. neutrophils, CD4<sup>+</sup> and CD8<sup>+</sup> T-cells). Acute inflammation in the form of substantial neutrophilia was due to the last LPS administration, whereas the observed eosinophilia and elevated counts of mast cell populations, CD4<sup>+</sup> and CD8<sup>+</sup> T-cells were due to the cumulative effects of LPS and elastase. The nature of COPD-associated inflammation in mast cell deficient mice was investigated in two experiments. Our first experiment suggested a mild protective role of mast cells, a finding not reproduced in the second experiment possibly due to expired elastase. Our study suggests that mast cells are not required for COPD-associated inflammation.

## **Popular science summary:**

Chronic Obstructive Pulmonary Disease (COPD) is a life threatening, underdiagnosed chronic inflammatory lung condition with increasing global prevalence. COPD is caused mainly by cigarette smoking in high income countries and biomass burning in low to middle income countries. COPD is on-track to be the third leading cause of death in 2020, the mortality of which is surpassed only by cardiovascular disease and cancer<sup>1</sup>. In Sweden, approximately 400-700,000 people have COPD<sup>2</sup>. Common symptoms include difficulty breathing, persistent cough, mucus overproduction and wheezing. Patients living with COPD experience an accelerated decline in lung function, a lower quality of life and are more likely to develop respiratory infections and co-occurring conditions such as heart disease and depression<sup>3</sup>.

Mast cells (MCs) are rare immune cells found in tissues of the body that face the external environment. These cells are highly involved in allergy and asthma. Increased counts of mast cells are common in the lungs of COPD patients, and evidence suggests that mast cells may be involved in COPD development<sup>4,5</sup>. Experimental mouse models can mimic human COPD and have been successfully used to better understand the disease in humans. The aim of my project was to investigate the pattern of inflammatory response in a mouse model of COPD-associated inflammation. The COPD-like inflammation in the lungs of mice were assessed using a technique known as flow cytometry. A genetically modified strain of mice that lack mast cells was compared to normal mice that have mast cells. In our first experiment, we observed that mice that lacked mast cells had less inflammation than the normal mice. However, when we repeated the experiment a second time, we could not find a difference in COPD-like inflammation between the mice that lacked mast cells and the normal mice. Thus, we could not find a consistent role of mast cells in the experimental model of COPD.

## §1: Introduction

### §1.1: Chronic Obstructive Pulmonary Disease (COPD)

COPD is a chronic lung disease, which causes breathing difficulties and respiratory symptoms especially in an aging population. COPD is a disease primarily affecting the lungs, a complex organ comprised of hundreds of millions of microscopic air sacs called alveoli. The World Health Organization (WHO) defines COPD as a lung disease characterized by chronic obstruction of lung airflow that interferes with normal breathing and is not fully reversible. The more familiar terms 'chronic bronchitis' and 'emphysema' are no longer used, but are now included within the COPD diagnosis. COPD is not simply a "smoker's cough" but a complex, under-diagnosed and life-threatening lung disease<sup>6</sup>. The latest figures from large scale epidemiological studies such as the Global Burden of Disease (GBD) and Burden of Obstructive Lung Diseases (BOLD) estimated that there were 384 million cases worldwide causing 3.2 million annual deaths in 2017. The estimated global prevalence of COPD in 2017 was 11.7% among individuals aged 40 or older (95% CI 8.4%-15.0%), and by 2060 it is predicted that COPD will cause 5.6 million deaths annually<sup>1,7</sup>. COPD is projected to be the third leading cause of death globally in 2020<sup>3</sup>, with a mortality surpassed only by cancer and cardiovascular diseases<sup>1,8</sup>. In Europe alone, the healthcare, disability and premature death associated with this condition result in an estimated annual economic burden of ~141 billion euros<sup>9</sup>. COPD is predominantly caused by cigarette smoking in developed countries and exposure to biomass burning in developing countries where 90% of COPD deaths occur<sup>10-13</sup>. Patients with COPD experience symptoms such as shortness of breath, cough, mucous hypersecretion and reduction of lung function with hallmarks of chronic airway inflammation (bronchitis) and emphysema<sup>14,15</sup>. Some genetic factors, such as alpha-1 antitrypsin deficiency (AATD) which is common in European Caucasians, and genetic variants encoding matrix metalloprotease-12 (MMP-12) have been implicated in COPD development<sup>16,17</sup>. Elastase is an important factor in COPD, highlighted by the role of alpha-1 antitrypsin in inhibiting neutrophil elastase and the increased risk of developing COPD in AATD patients<sup>18,19</sup>. Moreover, neutrophil elastase knockout mice are protected from emphysema induced by cigarette smoke exposure<sup>20</sup>. The role of a protease-antiprotease imbalance in pathogenesis is further complicated by the recent evidence of exosomes associating with neutrophil elastase, and that transplanting exosomes from COPD patients into mice induces emphysema rapidly<sup>21</sup>.

Although COPD occurs in a variety of clinical endotypes, all forms of COPD usually involve alveolar wall destruction (i.e. emphysema), small airways disease, pulmonary inflammation, and mucous hypersecretion. Currently, only two blood tests are used for identifying endotypes of COPD: AATD testing and blood eosinophilia<sup>22</sup>. However, COPD pathogenesis remains poorly understood.

The strong association of COPD with comorbidities such as hypertension, cardiovascular disease, lung cancer, and diabetes implicates COPD as the pulmonary element of a systemic and multimorbid syndrome<sup>8,23</sup>. An exacerbation of COPD is defined as an acute worsening of respiratory symptoms, often caused by respiratory tract infections that are prevented or managed via vaccination, antibiotics, as well as pharmacological and non-pharmacological (anti-inflammatory, surgical, oxygen, pulmonary, and prophylactic) therapies<sup>3,24</sup>. Between 30-50% of COPD exacerbations are caused by bacterial infection, with *non-typable Haemophilus influenzae*, *S. pneumoniae*, *Moraxella catarrhalis*, and *Chlamydia pneumoniae* being the most common, and 30% are caused by viral infections such as influenza virus, respiratory syncytial virus, and rhinovirus<sup>24–26</sup>. Modern COPD management that aims to prevent exacerbations involves inhaled long acting muscarinic agonists (LAMA),  $\beta$ -2 agonists (LABA), inhaled corticosteroid (ICS) therapies to modify small airway cholinergic tone, reduce inflammation and symptoms. Nonetheless, COPD remains a deadly, incurable disease.

Despite COPD being a heterogenous disease, distinctive inflammatory responses and location in the peripheral (lower) airways and lung parenchyma (elastin-rich portion of lung involved in gas transfer) have been described<sup>27</sup>. The infiltrating cells are primarily composed of neutrophils, macrophages and T-cells<sup>23</sup>. As expected, the inflammatory response within COPD involves innate and adaptive immunity linked by dendritic cell activation<sup>28</sup>. In fact, COPD severity has been associated with the level of inflammatory lung infiltration, including mast cells<sup>4,23</sup>. The nature of inflammation in COPD differs from that seen in other chronic lung diseases, such as asthma<sup>27</sup>. Immunological mechanisms thought to contribute to COPD are summarized in **Figure 1**:

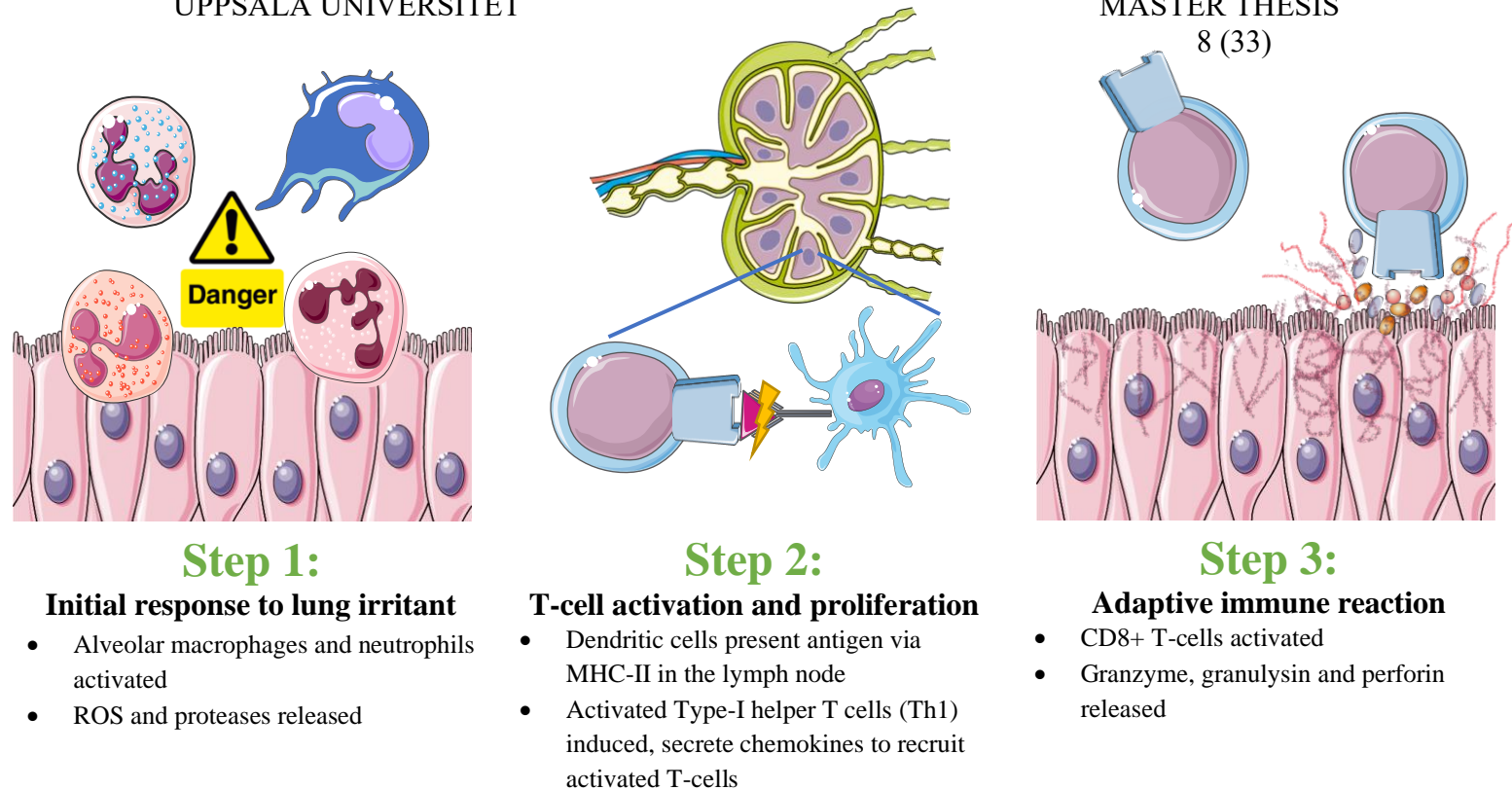


### Figure 1 Immunological mechanisms leading to COPD

**Step 1:** The inflammatory process begins with exposure to lung irritants, such as cigarette smoke (CS). A puff of CS contains  $\geq 5,000$  components, including  $\geq 70$  carcinogens, LPS, and  $10^{14}$  free radicals<sup>12,29</sup>. This leads to lung epithelial cell injury, and thus danger associated molecular patterns ‘DAMPs’ are released into the microenvironment. DAMPs are recognized by pattern recognizing receptors (PRRs) on innate immune system cells, which initiate immune responses against injured tissues. Increased numbers of activated neutrophils and alveolar macrophages creates a proinflammatory environment, which includes proteases that damage extracellular matrix and alveolar wall components (i.e. elastin, known to be chemotactic to monocytes<sup>30</sup>).

**Step 2:** Immature dendritic cells (DCs) alert the adaptive immune system to pathogens or tissue injury. DCs mature upon binding ligands (i.e. DAMPs) to Toll-like receptors (TLR). Mature DCs highly express class II major histocompatibility complex (MHC) molecules together with costimulatory molecules CD80/86, which directs them to lymph nodes (LN). In the LN, DCs activate T-cells via MHC-II and enables T-cell recruitment to the lung via inducing expression of tissue specific chemokine receptors<sup>31</sup>.

**Step 3:** The cytotoxic CD8+ T-cells are the principal cells in lung parenchyma in patients with COPD, and increases of CD8+ T-cells are correlated with increases of airflow obstruction and emphysema<sup>32,33</sup>.

How lung irritants such as CS activate the immune system is poorly understood. The “Danger hypothesis” is a plausible explanation as to how innate immunity may be involved in COPD pathogenesis<sup>31</sup>. The Danger hypothesis proposes that cellular damage and subsequent danger associated molecular patterns (DAMPs), not a microbe itself, alert the immune system to a potential threat. Epithelial cell injury in COPD has been shown to trigger pro-inflammatory TLR2 and TLR4 pathways<sup>34,35</sup>. Moreover, Asthma, COPD, and asthma-COPD overlap patients have been shown to each exhibit distinct DAMP release profiles<sup>36</sup>.



Epigenetic changes, age-related remodeling, oxidative stress, apoptosis, auto-immunity, adaptive immunity, resolution of inflammation, viral and bacterial infections promoting exacerbations have also been implicated in the pathogenesis of COPD<sup>23,31,37</sup>. The chronic immune reactions in COPD development may lead to the depletion of immune function over time, and patients with COPD experience three to six fold higher risk of *Streptococcus pneumoniae*-induced pneumonia<sup>38</sup>.

### §1.2: Mouse models of COPD

There are a variety of experimental animal models of COPD. Mouse models are particularly useful due to a similar immune system relative to humans, availability of genetically modified strains, and relative ease of use. Experimental COPD models commonly involve exposure to cigarette smoke (CS), lipopolysaccharide (LPS, bacterial endotoxin), and elastase, either alone or in combinations<sup>39</sup>. The combination of LPS/elastase has been well characterized for more than 3 decades, and has shown to yield more dramatic alterations in inflammatory changes, lung function, and histology than either agent independently<sup>40</sup>. These methods aim to artificially mimic aspects of human COPD such as goblet cell metaplasia, airway remodeling (e.g. increased airway thickness, lung compliance, and total lung volume), and recruitment of innate immune cells (e.g. neutrophilia, transient eosinophilia)<sup>24,41</sup>. Lung function in animal models of COPD can be measured with spirometry-like measurements such as forced expiratory capacity (defined as the ratio of forced expiratory volume in 100 milliseconds and forced vital capacity (FEV<sub>100</sub>/FVC), total lung capacity (TLC), lung resistance (R<sub>L</sub>) and dynamic compliance (C<sub>L</sub>) in mouse models of COPD.

Mouse models of COPD involving CS often require 6 months of inhalation, though refined models can produce emphysema and other hallmarks of COPD in 8 weeks-time. CS models reliably mimic COPD associated lung pathologies e.g. emphysematous destruction, airway fibrosis, cardiovascular pathologies, corticosteroid resistance, parenchymal inflammation, reduced infection clearance and increased infiltrates of neutrophils, macrophages and CD8<sup>+</sup> T-cells seen in humans<sup>40</sup>. However, CS induced models of COPD have not shown reliably mimic several aspects of the disease e.g. increased airway resistance, small airway obstruction or goblet cell metaplasia<sup>42</sup>.

Treatments with LPS/elastase induce features of COPD-like disease in mice such as emphysema, lung inflammation, airway remodeling, loss of lung elasticity, mucous hypertrophy, and immunological signatures (increased neutrophils, T and B cells, lymphocytes, monocytes, macrophages, in alveoli and airways). Moreover, pulmonary mechanics and inflammatory conditions seen in human COPD such as increases in IL-1 $\beta$ , IL-6, TNF- $\alpha$ , and CXCL2 last up to 8 weeks after i.n. LPS/elastase inoculation<sup>41</sup>. Nonetheless, LPS/elastase models oversimplify COPD pathogenesis and cannot fully replicate the true intricacies of pathology and pathogenesis within human COPD, such as irreversible lung damage or increased ratios of CD8<sup>+</sup>/CD4<sup>+</sup> T cell populations<sup>39–42</sup>. In animal models of COPD similar to the protocol used in our experiments, it has been estimated that 20% of parenchymal tissue loss and subsequent emphysema is due to elastase administration and 80% due to the host inflammatory response<sup>43</sup>.

The modeling of pulmonary disease in mice has been successfully used for decades, though physiological and anatomical differences must be considered between mouse and human lungs when interpreting the results. Mouse lung morphology is distinct from that of humans, with mice having four lobes (cranial, middle, caudal, and accessory, which is often subdivided into intermediate accessory and diaphragmatic lobes) in the right lung and a single lobed left lung, as opposed to humans three lobes (upper, middle, lower) in the right lung and two lobes (upper and lower) in the left lung<sup>44</sup>. Human lungs begin dichotomous branching at the trachea into both bronchioles and bronchi over 23 generations of branching into approximately 500 million alveoli, whereas branching of conducting airways in mice is monopodial<sup>45–47</sup>. Additionally, mice exhibit strain-specific airway variation and have a greater proportion of lung parenchyma in airway tissue relative to humans<sup>40</sup>.

### **§1.3: Mast cells**

Mast cells (MCs) were described as early as 1863 by Dr. von Recklinghausen, though the now canonical term “mastzellen” was coined by Dr. Paul Ehrlich in 1878<sup>48</sup>. MC-like cells have been described in invertebrate chordates, thus their role as sentinel immune cells pre-dates adaptive immunity by 500 million years<sup>49</sup>. MCs are long-lived tissue-resident cells found in all human vascularized tissues except the central nervous system and retina, and the proteome of MCs is evolutionarily conserved among mice and humans<sup>50,51</sup>. MCs are hematopoietic cells

belonging to the myeloid lineage. They have distinct development from granulocytes and develop from bone marrow or yolk sac-derived mast cell progenitors (MCp)<sup>51</sup>. MCp circulate as CD34<sup>+</sup> c-kit<sup>+</sup> FcεRI<sup>+</sup> cells in the blood, and upon localization in peripheral tissues MCp mature into mature mast cells (mMC) where reversible differentiation into phenotypes based on protease content occurs<sup>52</sup>. Human and mouse mast cells are classified into two major phenotypes: connective tissue mast cells (CTMCs) expressing tryptase and chymase (known as MC<sub>TC</sub> in humans) and mucosal mast cells (MMC<sub>s</sub>) expressing tryptase only (MC<sub>T</sub> in humans)<sup>50,52,53</sup>.

The classical and best understood mechanism of MC activation is via cross-linking of IgE bearing antigen with the high-affinity IgE receptor FcεRI. MCs can also be activated by a wide variety of other means, e.g. Mas-related G-protein coupled receptor member X2 (MRGPRX2), changes in osmolarity, complement anaphylatoxins C3a and C5a, and inflammasome activators and toll-like receptors (TLRs)<sup>54,55</sup>. Indeed, MCs are well equipped for early detection and battle against a wide variety of potential threats e.g. bacteria, viruses, venom and parasites<sup>56</sup>. Many aspects of MC function e.g. regulatory and activation pathways remain poorly understood<sup>57</sup>.

The cytoplasm of MCs contains approximately 50-200 large granules that are released upon activation, with the capability to re-granulate and remain functional<sup>58</sup>. MC degranulation involves rapid release of vasoactive amines such as histamine and serotonin (5-HT, 5-hydroxytryptamine), lysosomal hydrolases (i.e. β-hexosaminidase), proteases (tryptase, chymase, cathepsins C and G) and serglycin proteoglycans from metachromatic granules. After MC activation, MCs can also rapidly generate eicosanoids (leukotrienes and prostaglandins) and synthesize de-novo over 30 chemokines and cytokines<sup>56,59–61</sup>.

Diseases associated with MC dysfunction include mastocytosis and autoimmune diseases such as multiple sclerosis, cancer, and atherosclerosis<sup>62–65</sup>. MCs are also strongly implicated in allergic asthma, another inflammatory lung disease with distinct inflammatory signatures, immunological mechanisms, and disease management. Furthermore, MCs are thought to participate in lung injury healing, blood coagulation, maintaining vascular homeostasis, cell proliferation, tissue remodeling, phagocytizing bacteria, and releasing nuclear DNA to form antimicrobial extracellular traps (MCETs, similar to neutrophil extracellular traps “NETs”)<sup>66,67</sup>. The panoply of human mast cells receptors and respective ligands are described in Figure 2.

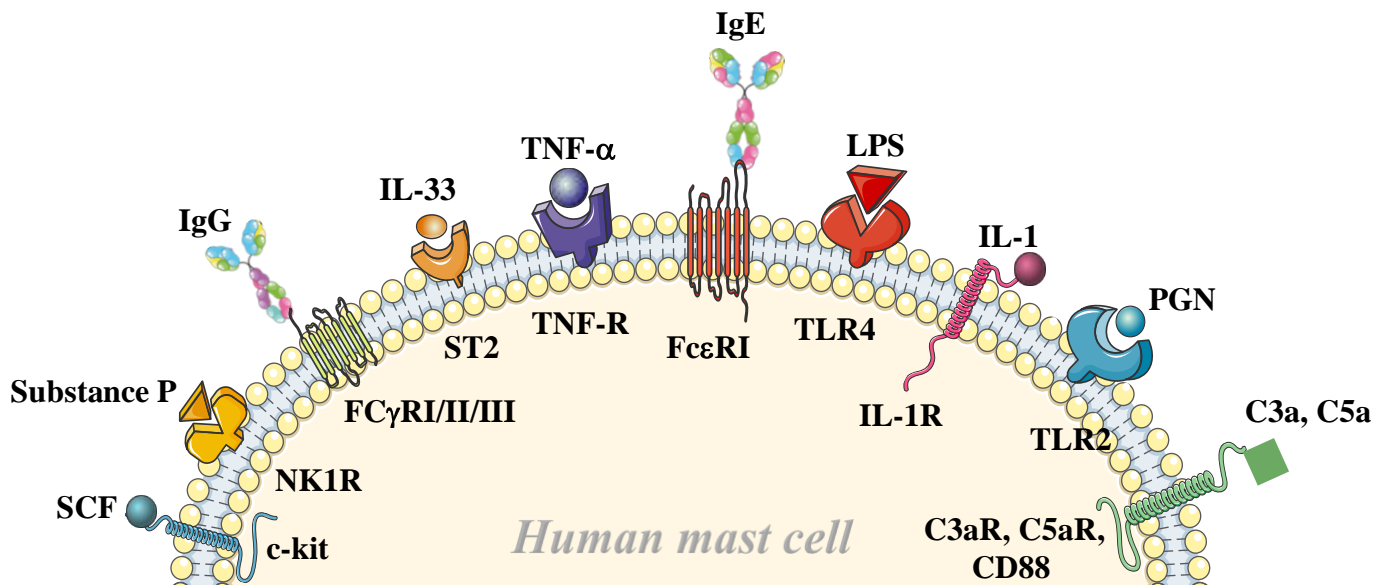


**Figure 2: Non-comprehensive list of human mast cell receptors and ligands**

Mast cells can respond to e.g stem cell factor (SCF), neuropeptides (i.e. substance P), IgG, cytokines, IgE, LPS, anaphylatoxins (C3a, C5a), peptidoglycan (PGN) and purinergic signals (adenosine, ATP) by expressing receptors depicted. MCs have demonstrated protective effects against parasites, bacteria, venom and are implicated in pseudo-allergic reactions to opioids<sup>68</sup>. Downstream effects include degranulation, G-protein coupled receptor (GPCR) signaling, gene transcription, NF- $\kappa$ B signaling, de-novo synthesis, and secretion of exosomes.

MCs are common in inflammatory infiltrates in the lungs of COPD patients, and existing evidence suggests that MCs could also be involved in COPD development<sup>4,5</sup>. Inflammatory conditions such as asthma have been shown to increase recruitment of MCs into the lungs<sup>52,69,70</sup>. In COPD with centrilobular emphysema, increased numbers of MCs correlate with decreased respiratory performance, increased airway remodeling and emphysema<sup>4,40,71</sup>.

The role of mast cell proteases in COPD has been experimentally tested by subjecting mice lacking mMCP-6 (the major secreted murine MC-specific tryptase) to a COPD model<sup>40</sup>. Indeed, mMCP-6 deficient mice exhibited reduced COPD-like pulmonary inflammation and similar lung function relative to wild-type controls<sup>40</sup>. Both recombinant mMCP-6 and human ortholog hTryptase- $\beta$  have been shown in vitro to induce recruitment of macrophages and increase expression of cytokines and chemokines<sup>40,72</sup>. In summary, there is increasing evidence that MCs have roles in physiological and pathophysiological processes which govern chronic lung disorders. Thus, MCs could potentially be involved in COPD pathogenesis, and it is vital to address the contribution of MCs to this disease as a whole. In my master project, I used a mast cell-deficient mouse strain to interrogate how mast cells contribute to COPD-associated pulmonary inflammation.

## **Aim**

The aim of my thesis is to determine whether mast cells play a role in pulmonary inflammation associated with COPD.

## §2: Methods

### Ethics

All procedures and experiments were approved by the Uppsala Regional Ethics Review Board under an ethical permit (No. 5.8.18-0527/2018) in accordance with Directive 2010/63/EU and Swedish Legislation (Djurskyddslagen 1988:534, 539; SJVFS 2012:26, Saknr. L150)

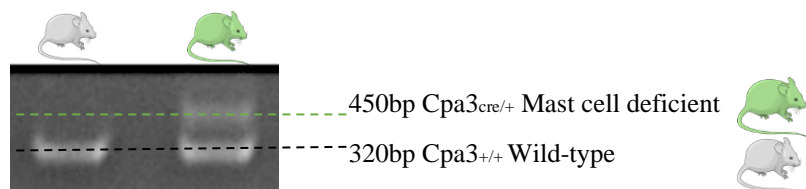
#### §2.1: Mice

Female mice (8-10 weeks of age; Balb/c-JBomTac) were housed at the National Veterinary Institute (Statens veterinärmedicinska anstalt, SVA). All animals had ad libitum access to food and water under a 12-hour light/dark cycle at 22 °C. All procedures and experiments were approved by the Uppsala research animal ethics committee in accordance with an ethical permit (No. 5.8.18-0527/2018).

#### §2.2: Genotyping of Cpa3<sup>Cre/+</sup> mice

Mast cell deficient Cpa3<sup>Cre/+</sup> mice were used in our experiments. Cpa3<sup>Cre/+</sup> utilized an inserted cre-recombinase gene within mast cell carboxypeptidase A3 (CPA3), resulting in genotoxic overexpression of cre-recombinase in Cpa3 expressing cells, leading to a deficiency in mast cells and a reduction of basophils<sup>73</sup>. Ear biopsies were obtained and stored at 4 °C. For DNA extraction, 40 mL of 1x Modified Gitschier Buffer with 1% β-Mercapto ethanol and 0.5% Triton X-100 was added, and endogenous enzymes were heat inactivated at 95 °C for 5 minutes. Next, 1 mL proteinase K was added to each sample. After incubation for 45 minutes at 55 °C, Proteinase K was heat inactivated at 95 °C for 10 minutes, then samples were centrifuged to remove tissue residues for 3 minutes at 13,000rpm. Supernatant (25 µL) was transferred into new tubes and stored at -20 °C until polymerase chain reaction (PCR). The genotype of mice was determined by PCR assay yielding 320bp (Cpa3<sup>+/+</sup>) and 450bp (Cpa3<sup>Cre/+</sup>) products, shown below.

The PCR reaction was prepared as illustrated in the table below



#### Sequences of oligonucleotide primers:

**Common:** 5' GGA CTG TTC ATC CCC AGG AAC C 3'

**WT:** 5' CTG GCG TGC TTT TCA TTC TGG 3'

**KI:** 5' GTC CGG ACA CGC TGA ACT TG 3'

The PCR was performed using the described steps below:

- Step 1: 94 °C 2 minutes
  - Step 2: 94 °C 20 seconds
  - Step 3: 62 °C 30 seconds
  - Step 4: 72 °C 30 seconds
  - Step 5: 72 °C 5 minutes
  - Step 6: 4 °C indefinite cold hold
- } 34 cycles

Per PCR reaction:	
Reagent	Quantity (mL)
H <sub>2</sub> O	14.3
Oligos	1
10X PCR buffer	2.5
dNTP	2.5
MgCl <sub>2</sub>	1.5
Taq polymerase	0.2
DNA template	1
<b>Final Volume</b>	<b>25</b>

#### Reagents:

- ♦ Modified Gitschier Buffer (MGB)
    - 10X MGB
      - 670 mM Tris-HCL pH 8.8 – 6.7 mL 1 M Tris-HCL pH 8.8
      - 1.66 mM (NH<sub>4</sub>)<sub>2</sub>SO<sub>4</sub> – 1.66 mL 1 M (NH<sub>4</sub>)<sub>2</sub>SO<sub>4</sub>
      - 65 mM MgCl<sub>2</sub> – 650 mL 1 M MgCl<sub>2</sub>
      - 990 mL H<sub>2</sub>O
  - ♦ 1X MGB with 1% b-Mercapto ethanol and 0.5% Triton X-100
- 4 mL MGB 10X + 33.6 mL H<sub>2</sub>O + 0.4 mL b-Mercapto ethanol + 2 mL 10% Triton X-100

### §2.3: LPS/elastase protocol to induce COPD-like inflammation

Mice received weekly doses of intranasal (i.n.) 1.2 U of porcine pancreatic elastase (Cat. 324682, Sigma-Aldrich) and 7 µg of LPS from *Escherichia coli* O26:B6 (Cat. L8274, Sigma-Aldrich) in PBS, or 50 µl of PBS (vehicle control) as shown below in Figure 3. Lung and bronchoalveolar lavage fluid (BALF) collection were performed one, four or seven days after the last LPS dose.

#### §2.4: Bronchoalveolar lavage fluid

Mice were euthanized via cervical dislocation. The lungs were lavaged with 1 mL ice-cold PBS and stored at 4 °C. Bronchioalveolar lavage fluid (BALF) was centrifuged 15,900 rcf at 4 °C and supernatants were separated and stored at -20 °C for future analysis. Erythrocytes were eliminated from the cell pellet by 30 seconds incubation with 50 µL cell lysis solution (150 mM NH<sub>4</sub>Cl, 10 mM NaHCO<sub>3</sub> and 1.26 mM EDTA) and 1mL FACS buffer (PBS w/ 2% fetal calf serum) was added to stop the reaction and cells were resuspended in FACS buffer. Viable cells were counted in a Bürker hemocytometer using Trypan blue staining (Cat. T8154, Sigma-Aldrich) and viewed under a Leitz Laborlux S microscope (Leica Microsystems)

#### §2.5: Lung digestion

After BALF extraction, whole lung specimens were collected and digested using a Lung Dissociation Kit (Cat. 130-095-927, Miltenyi Biotec). In summary, lung tissue was homogenized using a surgical blade and incubated (30 minutes, 37 °C) with digestion enzymes in a gentleMACS Octo Dissociator with Heaters (Miltenyi Biotec) using program 37C\_m\_LDK\_1). Undigested tissue and lung epithelium were removed from the resulting cell suspension using a Percoll gradient (Percoll 44% in RPMI media). Cells were resuspended in FACS buffer, erythrocytes were lysed as described in §2.4, and viable cells counted as described above.

##### Cell isolation reagents:

- Lysis buffer
  - 150 mM NH<sub>4</sub>Cl, 9.5 mM NaHCO<sub>3</sub>, and 1.2 mM EDTA (pH 7.4)
- FACS Buffer
  - 2% heat inactivated fetal calf serum (FCS) in 1X PBS (pH 7.4)
- Percoll 44%
  - 22mL 100% Percoll, 28mL complete RPMI
- Lung dissociation enzymes (Miltenyi Biotec, per lung, V<sub>f</sub> = 2515 µL)
  - 2.4 mL Buffer S
  - 15 µL Solution A
  - 100 µL Solution D

#### §2.6: Flow cytometry

Single cell suspensions were prepared for flow cytometric analysis as follows: Lung homogenate samples were brought to the same 2 mL volume with FACS buffer after pooling approximately 5 million cells for each FcεRI and ST2 isotype and unstained control. Samples were centrifuged at 400 g for 5 minutes and supernatant extracted for storage at -80 °C for



future analysis. Cell samples were then incubated with antibody (see **Table 1**) at 4 °C protected from light for 30 minutes. Cells were washed twice with 3 mL chilled FACS buffer with intermediate centrifugation at 400 g for 5 minutes. Samples were resuspended in 500 µL FACS buffer and protected from light at 4 °C until acquisition. Finally, 7 million lung homogenate cells were acquired for analysis via flow cytometry. BALF single cell suspensions were prepared in a similar manner: BALF samples were centrifugated at 15,900 rcf for 3 minutes and supernatant was collected in separate tube to be stored at -80 °C for future analysis. Erythrocytes were lysed as described in §2.4 followed by a centrifugation at 15,900 rcf for 3 minutes and resuspension in 500 µL chilled FACS buffer. Prior to staining, 50 µL from two high yield BALF samples was pooled for the unstained control. Samples were then incubated with antibodies (see **Table 1**) for 30 minutes at 4 °C protected from light. Then, samples were resuspended in 500 µL FACS buffer and protected from light at 4 °C until flow cytometric acquisition. Finally, 50,000 BALF cells were acquired for analysis. Flow cytometric analysis was performed using an LSRFortessa (BD biosciences) flow cytometer equipped with 5 lasers (355, 405, 488, 561, 640nm) within BioVis facilities at Uppsala University. Data was analyzed with FlowJo v.10 software (BD Biosciences). Gating strategies are shown in Results section (**Figures 4, 5, 8**) with population hierarchies shown below.

**BAL cell populations:**

Eosinophils: CD45<sup>+</sup> CD11c<sup>-</sup> SiglecF<sup>+</sup> cells

Alveolar Macrophages: CD45<sup>+</sup> CD11c<sup>+</sup> SiglecF<sup>+</sup> cells

Neutrophils: CD45<sup>+</sup> CD11c<sup>-</sup> SiglecF<sup>-</sup> CD11b<sup>+</sup> Ly6G<sup>+</sup> cells

T-cells: CD45<sup>+</sup> CD11c<sup>-</sup> SiglecF<sup>-</sup> CD11b<sup>+</sup> Ly6G<sup>-</sup> CD4<sup>+</sup> or CD8<sup>+</sup> cells

**Lung homogenate cell populations:**

Mast cell progenitor (MCp): CD45<sup>+</sup> Lin<sup>-</sup> c-kit<sup>+</sup> FcεRI<sup>+</sup> CD11b<sup>-</sup> ST2<sup>+</sup> Intβ7<sup>hi</sup> cells

Mature mast cell (MMC): CD45<sup>+</sup> Lin<sup>-</sup> c-kit<sup>+</sup> FcεRI<sup>+</sup> CD11b<sup>-</sup> ST2<sup>+</sup> Intβ7<sup>lo</sup> cells

Basophils: CD45<sup>+</sup> Lin<sup>-</sup> c-kit<sup>-</sup> FcεRI<sup>+</sup> CD49b<sup>+</sup> cells

<b>Table 1: Antibody panels - Sourced from BD Biosciences</b>	
<b>BAL (1 µL antibody/sample)</b>	<b>Lung homogenate (1 µL antibody/sample)</b>
CD45 - Alexa700	CD45 - Alexa700
CD11c - PeCy7	CD3 - PE-Cy5
SiglecF - BV421	CD4 - PE-Cy5
DC11b - FITC	CD19 - PE-Cy5
Ly66 - BV605 (QD625)	B220 - PE-Cy5
CD3 - PE	TERII - PE-Cy5
CD4 - PeCy5	CD8 - PE-Cy5
CD8 - BV510	CD11b - PE-Cy5
	c-kit - PE-Cy7
	FcεRI - PE
	ST2 - BV421 or BV786 in basophil panel
	CD 16/32 - BV605 (QD605)
	CD49b - BV421
*5 µL antibody/sample	*Integrin-β7 - FITC

### §2.7: Statistics

For analysis of >three groups, the means were compared using analysis of variance (ANOVA), and along with Tukey's test for multiple pair-wise comparisons. Student's t-test was used when comparing two groups. A p-value <0.05 was considered a significant difference. Data was formatted and analyzed using Prism 8 software (GraphPad Software Inc.)

## §3: Results

### §3.1 Validation of COPD model

**Repeated doses of elastase and LPS over four weeks produced a model of COPD-like lung inflammation.**

To model COPD in mice, we administered intranasal (i.n.) inoculations of 1.2 U porcine pancreatic elastase (PPE) and 7  $\mu$ g LPS once a week for 4 weeks (**Figure 3**).

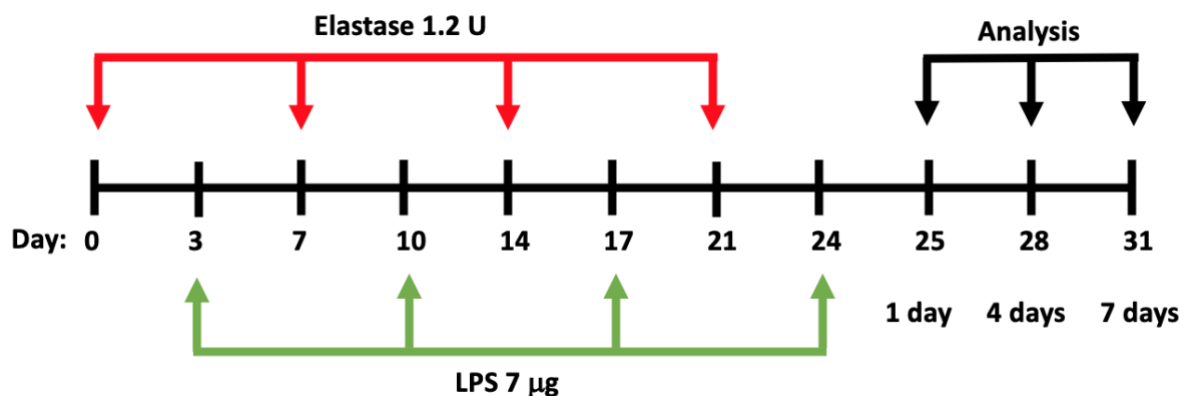
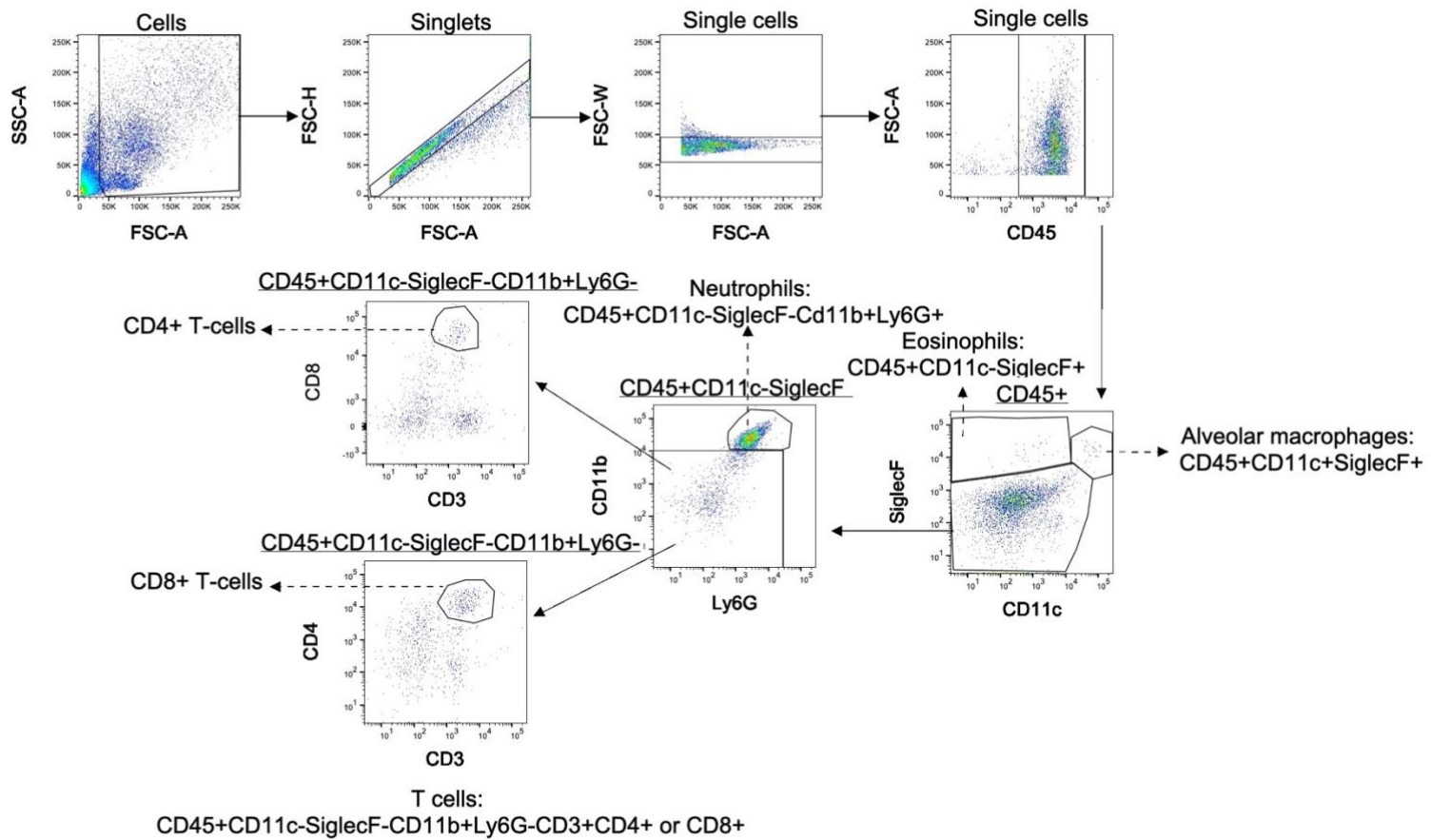


**Figure 3: The model of COPD-like inflammation.**

Mice received weekly intranasal (i.n.) doses of porcine pancreatic elastase (PPE) and of LPS as depicted. Control mice received PBS as a vehicle control. The mice were euthanized and lung and bronchoalveolar lavage fluid (BALF) collected one, four or seven days after the last LPS dose.

We investigated whether the elastase- and LPS-dependent COPD model induced signs of general lung inflammation, and whether mast cell numbers increased. Quantification of alveolar macrophages, eosinophils, neutrophils, and CD4<sup>+</sup> and CD8<sup>+</sup> T-cells was performed by flow cytometry using the gating strategy shown in **Figure 4A**. The protocol used in this study did not induce any significant increase in total BAL cell numbers or alveolar macrophages at any days investigated (**Figure 4B, C**). However, acute inflammation of the airways was characterized by neutrophilia on day 1 (**Figure 4E**), and a small increase in eosinophils (**Figure 4D**). The levels of neutrophils and eosinophils in BALF decreased on days 4 and 7. The number of CD4<sup>+</sup> T-cells were increased at all time points; however, we only saw a statistically significant increase 4 days after the final LPS treatment (**Figure 4F**). In contrast, CD8<sup>+</sup> T-cells increased on day 1, but decreased to a level that was comparable to control mice on later days (**Figure 4G**).

A.



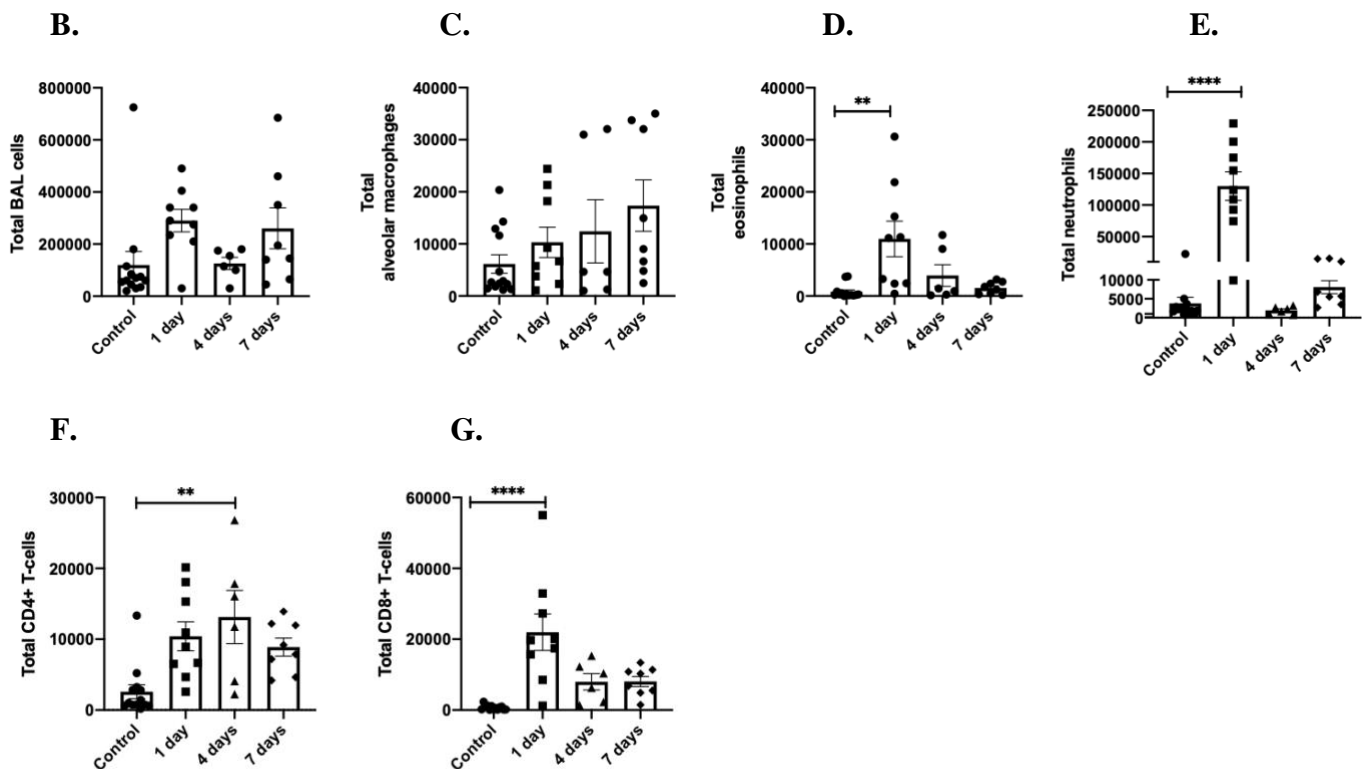


**Figure 4: COPD-like inflammation is induced by repeated intranasal doses of LPS and elastase.**

Mice were given intranasal doses of LPS and elastase to induce COPD-like inflammation. BALF was obtained 1, 4, and 7 days after the last LPS administration. (A) Gating strategy used to analyze BAL samples. (B) BAL cells were manually counted using a hemocytometer. Alveolar macrophages (C), Eosinophils (D), Neutrophils (E), and CD4<sup>+</sup> T-cells (F) and CD8<sup>+</sup> T-cells (G) were quantified by flow cytometry. Data shown are pooled from six experiments (two duplicate experiments per sampling day). Cell estimates are presented as mean  $\pm$  SEM with each individual value shown. Statistical significance was tested via one-way ANOVA followed by post-hoc Tukey test.  $P < 0.01 = **$ ,  $P < 0.0001 = ****$ .

To quantify mast cells and their progenitors, mouse lungs were homogenized. The resulting single cell suspension was manually counted using a hemocytometer and analyzed by flow cytometry using the gating strategy described in **Figure 5A**. The total lung cells increased in mice with COPD-like inflammation on days 1 and 7 but were at a similar level as control mice on day 4. (**Figure 5B**). The lung mast cell progenitors (MCP) increased 1 day after the last LPS administration but were at similar levels as in control mice when analyzed on days 4 and 7 (**Figure 5B**). In contrast, the number of total lung mast cells increased slightly at day 7 after the last LPS administration (**Figure 5D**).

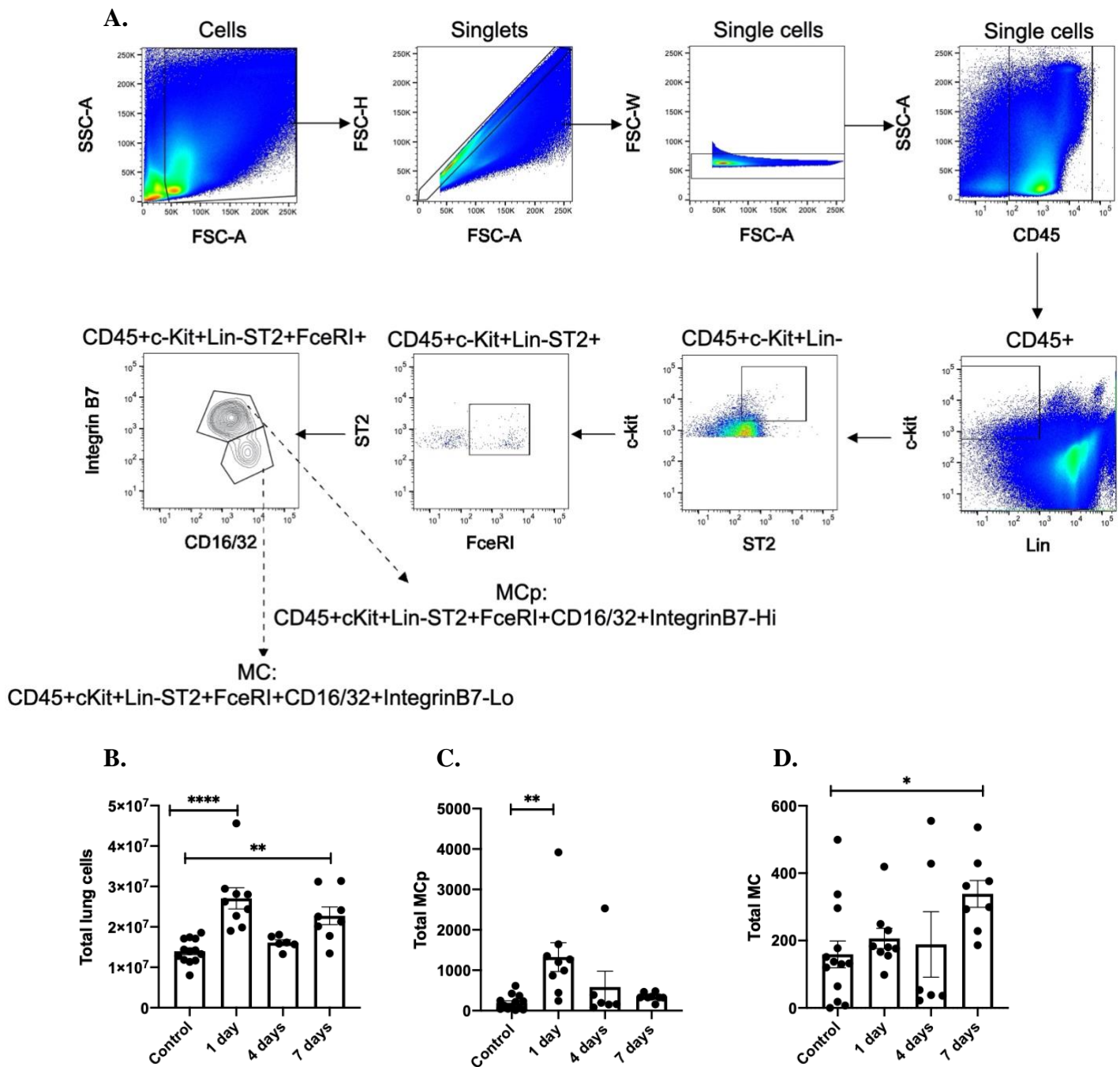


**Figure 5: Lung MCp increase transiently one day after the last LPS dose, whereas lung mast cells accumulate 7 days after the last LPS dose.**

Lung homogenates were obtained 1, 4, and 7 days after the last LPS administration and the indicated cell populations were quantified by flow cytometry. (A) Gating strategy for lung homogenate cells. Data shown represent the total number of lung cells (B), MCp (C) and mast cells (D) pooled from six experiments (two duplicate experiments per sampling day). Cell estimates are presented as mean  $\pm$  SEM with each value shown. Statistical significance was tested via one-way ANOVA followed by post-hoc Tukey test.  $P < 0.05 = *$ ,  $P < 0.01 = **$ ,  $P < 0.0001 = ****$ .

### §3.2 Mast cells appear not to be required for COPD-associated lung inflammation.

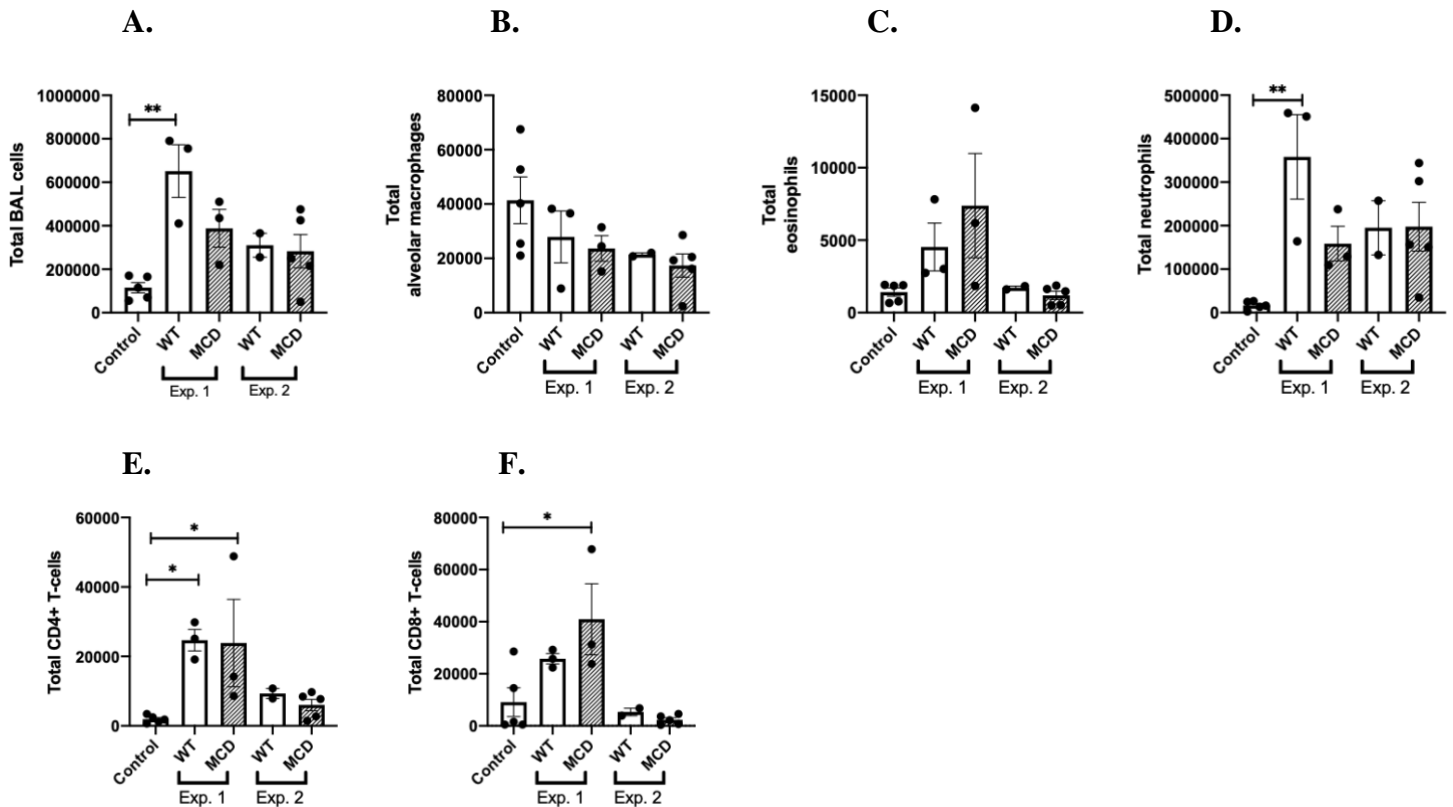


**Figure 6: Mast cells do not seem to play a role in COPD-like inflammation.**

Mast cell deficient (MCD) and wild-type (WT) mice were subjected to the COPD model and BALF was obtained 1 day after the last LPS administration. (A) BALF cells were manually counted using a hemocytometer. Alveolar macrophages (B), Eosinophils (C), Neutrophils (D), CD4+ T-cells (E), and CD8+ T-cells (F) were quantified by flow cytometry. Data shown represent two duplicate experiments with 3-5 mice per group shown separately with pooled controls (PBS treated). Cell estimates are presented as mean  $\pm$  SEM with each value shown. Statistical significance was tested via one-way ANOVA followed by post-hoc Tukey test.  $P<0.05=*$ ,  $P<0.01=**$ .

In order to determine the role of mast cells in COPD-associated inflammation, a strain of mast cell deficient (MCD) mice and their wild-type (WT) littermate controls were treated with the LPS/elastase protocol (Figure 3) or given PBS as vehicle controls. One day after the final LPS administration, BALF was analyzed for inflammatory cells and lung homogenates were analyzed to quantify mast cells and basophils by flow cytometry. Two experiments were performed, but due to the high variability observed we decided to plot them separately (Figure 6). In the first experiment (Exp. 1), MCD mice had lower numbers of BAL cells than their WT littermates, likely owing to less neutrophilia (Figure 6A, D). The number of alveolar

macrophages was similar in all tested groups (**Figure 6B**). Moreover, eosinophilia was only induced in Exp. 1, but there was no difference between genotypes (**Figure 6C**). An increase in CD4<sup>+</sup> T-cells was observed in both WT and MCD LPS/elastase-treated groups in Exp. 1, but not in the second experiment (**Figure 6E**). Similarly, the MCD mice had significantly more CD8<sup>+</sup> T-cells than the control group in Exp. 1, but not in Exp. 2 (**Figure 6F**).

### §3.3 A single intranasal dose of LPS induces an increase in total BALF cells, neutrophils, and CD4<sup>+</sup> T-cells.

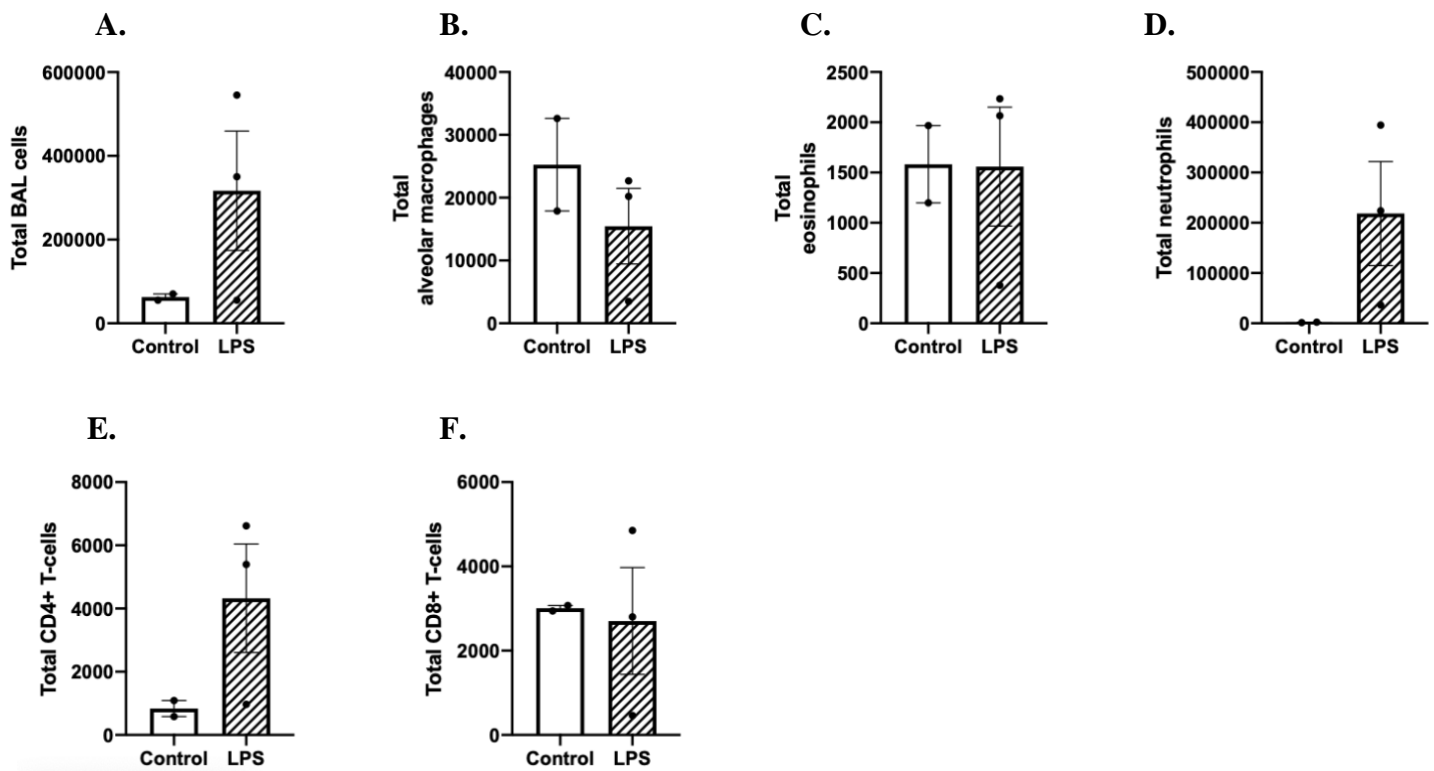


#### Figure 7: A single dose of LPS induces airway neutrophilia.

Mice were given 7  $\mu$ g LPS alone or PBS as a vehicle control. The following day, BALF was obtained and (A) total cells were manually counted by hemocytometer. The populations of alveolar macrophages (B), eosinophils (C), neutrophils (D), CD4<sup>+</sup> T-cells (E) and CD8<sup>+</sup> T-cells (F) were quantified by flow cytometry. Data shown represent a single experiment with 2-3 mice per group. Cell estimates are presented as mean  $\pm$  SEM with each value shown. Due to technical problems one control mouse could not be analyzed, and thus statistical analysis was not possible.

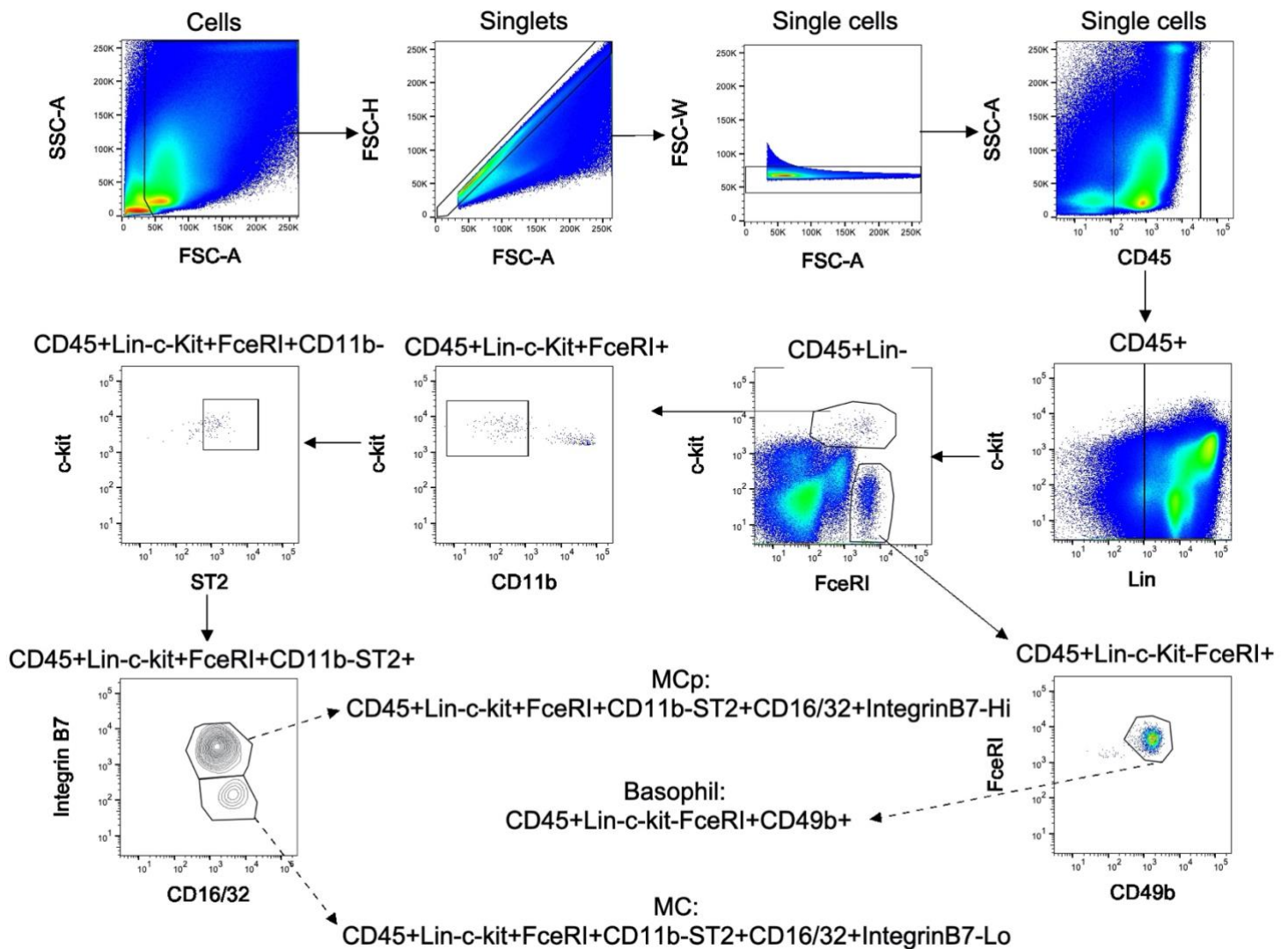
To evaluate the effect of LPS alone on lung inflammation, mice were given a single dose of LPS i.n. or an equal volume of PBS and analyzed one day after. In a single experiment, LPS induced a high number of BALF cells, neutrophils, and CD4<sup>+</sup> T-cells (**Figure 7A, D, E**).



However, no apparent changes in the total number of alveolar macrophages, eosinophils or CD8<sup>+</sup> T-cell were found (**Figure 7B, C, F**).

**Figure 8:**

**A.)**



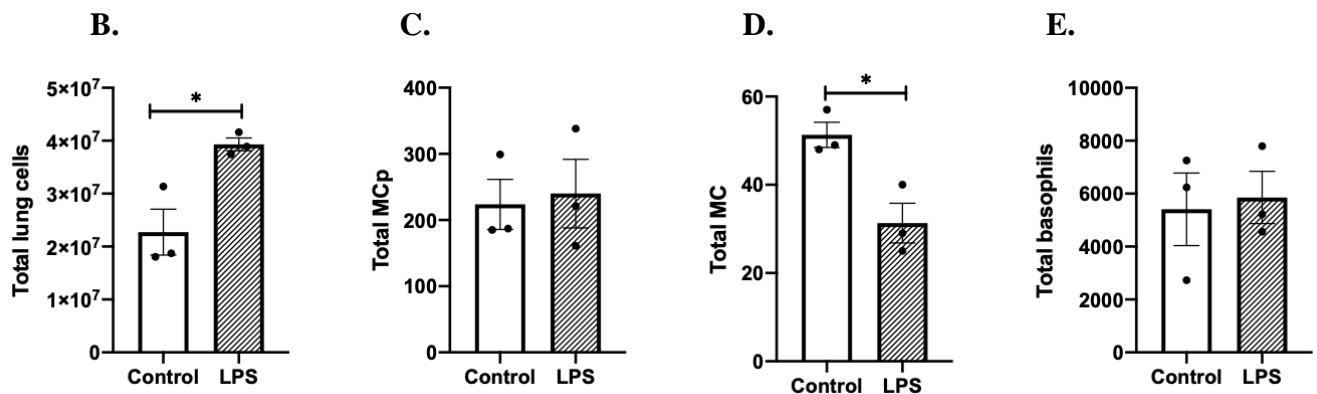


**Figure 8: A single dose of LPS does not induce an increase in lung MCp, mast cells or basophils.**

Mice were given a single dose of LPS or PBS i.n. One day later, their lungs were dissected, homogenized, and single cell suspension was prepared. (A) The gating strategy for quantification of MCp, mature mast cells (MC), and basophils. (B) Total lung homogenate cells were counted manually with a hemocytometer, while the MCp (C), MC (D), and basophils (E) were quantified by flow cytometry. Data shown represent a single experiment with 3 mice per group. Cell estimates are presented as mean  $\pm$  SEM with each value shown. Statistical significance was assessed using an unpaired Student's t-test, Confidence level = 95%, two-tailed P-value  $<0.05 = *$ .

To investigate whether a single dose of LPS was enough to induce a higher number of lung MCp, and to establish whether basophils could also be increased in this setting, lung homogenates were analyzed by flow cytometry following the gating strategy depicted in **Figure 8A**. Although LPS induced an increase in total lung cells (**Figure 8B**), no increase in lung MCp, mast cells, or basophils were observed (**Figure 8B-D**).

### §3.4 A single dose of intranasal elastase did not induce lung inflammation

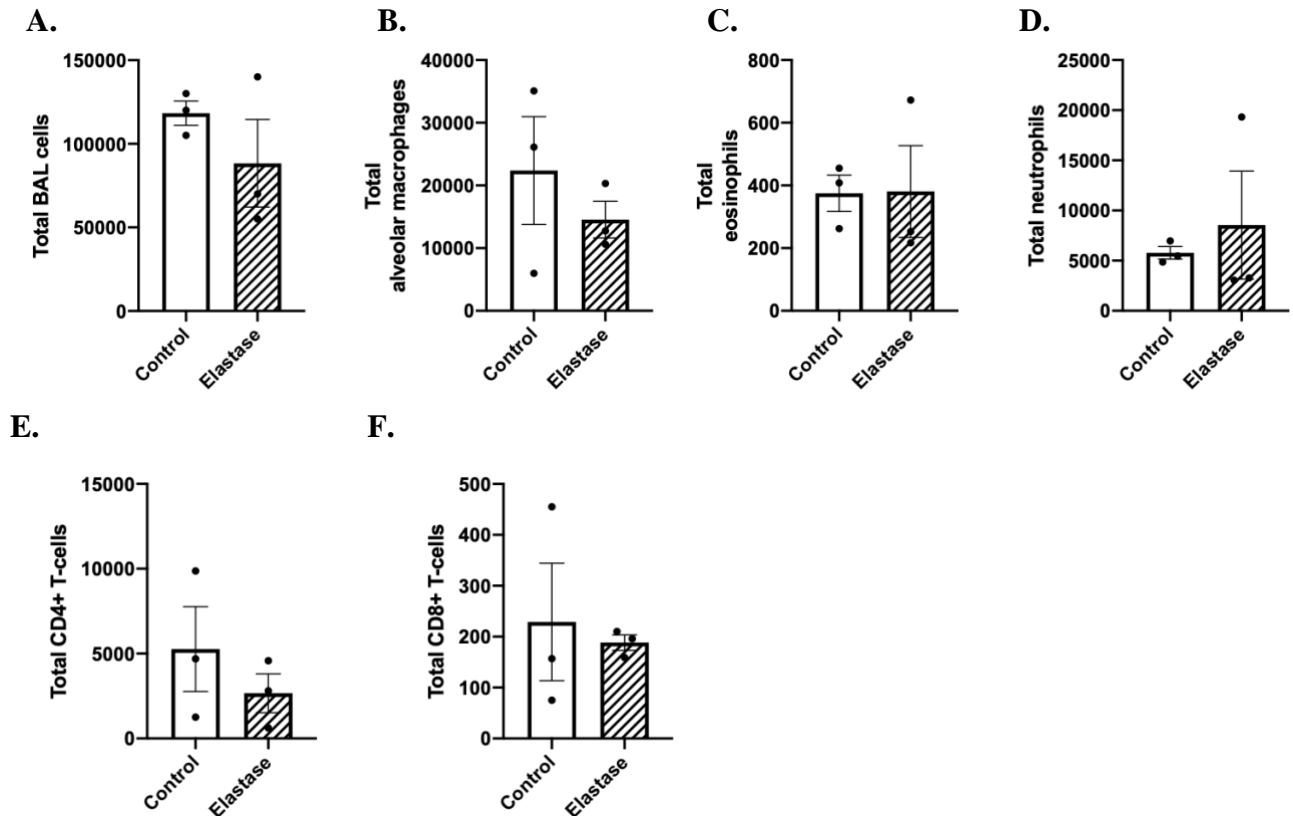


**Figure 9: A single dose of elastase did not cause signs of inflammation after 21 days.**

Mice were treated with a single i.n. dose of elastase or PBS as a control. After 21 days, BALF was collected, and (A) total cell counts were quantified manually with a hemocytometer. The total number of alveolar macrophages (B), eosinophils (C), neutrophils (D), CD4+ T-cells (E) and CD8+ T-cells (F) was determined by flow cytometry. Data shown represent a single experiment with 3 mice per group. Cell estimates are presented as mean ± SEM with each value shown. Statistical significance was tested using an unpaired Student's t-test.

A previous publication from Shibata *et al.* 2018 reported that a single dose of elastase causes COPD-like pathology characterized by cellular infiltration and emphysema after 21 days<sup>74</sup>. Thus, we wanted to test whether this protocol would induce a similar degree of inflammation as our LPS/elastase model of COPD-like inflammation. Mice were given a single dose of elastase or PBS as a control, and BALF was obtained 21 days after and analyzed for inflammatory cells by flow cytometry. There were no significant increases in total BAL cell, total alveolar macrophages, eosinophils, neutrophils, CD4+ or CD8+ T cells by the elastase treatment (Figure 9A-F).

## §4: Discussion

The primary objective of this thesis was to determine whether mast cells play a role in pulmonary inflammation associated with COPD. There are no standard models available in mice that can fully mimic the enormous complexity of COPD development in humans. Several research groups have employed refined CS-dependent models to induce COPD-like symptoms in animals, and indeed CS exposed mice develop emphysema and pulmonary inflammation. However, protocols involving CS require complicated exposures daily over long periods of time (usually months) and can only induce mild symptoms. Another accepted laboratory model consists of delivering elastase and LPS weekly for four weeks, which has been shown to cause more severe symptoms in less time. We subjected mice to an elastase and LPS-dependent COPD-like model (**Figure 3**) and evaluated the resulting pulmonary inflammation one, four, and seven days after the final LPS dose (**Figure 4** and **5**). In our experiments, we chose to use female mice for technical reasons: female mice of the same age have more consistent weight and they are less prone to fighting (wounds and skin infections would bias our results) than their male counterparts. Interestingly, sex differences in susceptibility to COPD have been described in humans, with female smokers having approximately 50% greater risk of developing COPD relative to males<sup>75,76</sup>. Similar sex differences have been described in mice. The exact reasons for this discrepancy are still unknown, though there is increasing evidence that women may have more active immune systems than men, potentially explaining why women are also disproportionately affected by autoimmune diseases<sup>77,78</sup>.

In agreement with previous publications and with the inflammatory response observed in COPD patients<sup>24</sup>, we found substantial neutrophilia and a statistically significant increase in CD4<sup>+</sup> and CD8<sup>+</sup> T-cells in BALF of treated mice at different time points in the COPD-like inflammation protocol (**Figure 4E-G**). However, we did not observe a statistically significant increase in alveolar macrophages (**Figure 4C**). In contrast, mice with COPD-like inflammation also had a small yet significant increase in eosinophils (**Figure 4D**). These results show both the benefits and the limitations of the model employed, and that the inflammatory response varied depending how many days after the final LPS dose analysis was performed.

Alterations in MC populations within inflammatory infiltrates of COPD patients have been described<sup>4</sup>, and we found that elastase and LPS-treated mice had a significant accumulation of MCp and mature mast cells 1 and 7 days after the final LPS dose, respectively (**Figure 5C-D**).

This prompted us to investigate a potential role for mast cells in COPD-associated pulmonary inflammation, but our experiments with MCD mice failed to reveal any significant phenotype (**Figure 6**). Nonetheless, our two MCD experiments had profoundly different results that we did not deem acceptable to pool together. The results of the first MCD experiment suggested a protective role for mast cells in COPD-associated pulmonary inflammation, while the second experiment failed to reproduce this trend (**Figure 6A**). These differences, however, could have been caused by an expired elastase, given that we performed our second experiment close to the enzyme's expiration date. New experiments with freshly prepared elastase and quantification of elastase activity using a chromogenic substrate are pending.

Finally, we wanted to determine whether a single dose of LPS or elastase could replicate the pulmonary inflammation observed in our experiments. Our data suggests that acute inflammation characterized by substantial neutrophilia (**4E**) and elevated counts of CD4<sup>+</sup> T-cells (**4F**) and appear to be due to the last dose of LPS (**7D, E**). The elevated infiltrating cells in lung homogenate samples (**4B**) may include alveolar macrophages and neutrophils, though this could be investigated using different cell panels in future experiments. The single LPS dose failed to cause eosinophilia, elevated counts of CD8<sup>+</sup> T-cells, MCp or mast cells (**Figure 7 C and F, Figure 8 C and D**) that was seen in our wild-type COPD experiment. Therefore, the effects of LPS and elastase used together accounted for eosinophilia and neutrophilia on day 1, increased CD4<sup>+</sup> T-cells on day 4, and increased CD8<sup>+</sup> T-cells on day 7 that were not observed in the single dose experiments. The antigen-specific response of  $\alpha\beta$  T-cells requires several days of activation, though rapid pro-inflammatory bystander activation of memory T-cells or  $\gamma\delta$  T-cells may explain the temporal trend observed<sup>79–81</sup>. This is consistent with previous research showing that the effects of LPS and elastase are synergistic and not additive<sup>41</sup>. Contrary to what had been previously reported in Shibata *et al.* 2018<sup>74</sup>, we did not observe any pulmonary inflammation in mice that were treated with a single dose of elastase after 21 days (**Figure 9**). Further validation of our model will require further experiments and may include the study of chronic inflammation beyond the 7-day period in our experiment, use of male mice or older mice, histology and serum analysis. The use of different antibody panels could be applied to investigate other immune cells e.g. natural killer (NK) cells or  $\gamma\delta$  T-cells by flow cytometry. The project covered in this thesis has helped validate an elastase and LPS-

dependent COPD-like model in mice, that can be used in order to further explore the potential roles of mast cells in human COPD.

## Acknowledgements

- ◆ Figures 1 and 2 were created with images derived from Servier Medical Art (smart.servier.com), which is licensed under a Creative Commons Attribution 3.0 Unported License.
- ◆ Laboratory protocols were derived from Standard Operating Procedures within Department of Immunology B9:3, IMBIM. Internal codes used: 017, 021, 022.
- ◆ This thesis would not be possible without the generous and excellent assistance of my supervisor, Jenny Hallgren Martinsson, PhD
- ◆ Project work was highly enjoyable under the skilled guidance of my patient lab supervisor, Eduardo Cárdenas, PhD
- ◆ A big thank you to my friends, family and my sambo Madeleine for all of your loving support in every step of my journey.

## References

1. GBD. Global, regional, and national age-sex-specific mortality for 282 causes of death in 195 countries and territories, 1980-2017: a systematic analysis for the Global Burden of Disease Study 2017. *Lancet* **392**, 1736–1788 (2018).
2. Nationella riktlinjer för vård vid astma och kroniskt obstruktiv lungsjukdom (KOL) - Socialstyrelsen. <https://www.socialstyrelsen.se/regler-och-riktlinjer/nationella-riktlinjer/slutliga-riktlinjer/astma-och-kol/>.
3. Gold Report 2020. *Global Initiative for Chronic Obstructive Lung Disease - GOLD* <https://goldcopd.org/gold-reports/>.
4. Andersson, C. K., Mori, M., Bjermer, L., Löfdahl, C.-G. & Erjefält, J. S. Alterations in lung mast cell populations in patients with chronic obstructive pulmonary disease. *Am. J. Respir. Crit. Care Med.* **181**, 206–217 (2010).
5. Mortaz, E., Folkerts, G. & Redegeld, F. Mast cells and COPD. *Pulm Pharmacol Ther* **24**, 367–372 (2011).
6. WHO | COPD: Definition. *WHO* <https://www.who.int/respiratory/copd/definition/en/>.
7. GBD 2013 Mortality and Causes of Death Collaborators. Global, regional, and national age–sex specific all-cause and cause-specific mortality for 240 causes of death, 1990–2013: a systematic analysis for the Global Burden of Disease Study 2013. *The Lancet* **385**, 117–171 (2015).
8. Eurostat. [https://ec.europa.eu/eurostat/statistics-explained/index.php?title=Causes\\_of\\_death\\_statistics](https://ec.europa.eu/eurostat/statistics-explained/index.php?title=Causes_of_death_statistics) (2016).
9. ERS. *The economic burden of lung disease - ERS* <https://www.erswhitebook.org/chapters/the-economic-burden-of-lung-disease/> (2013).
10. Adenro, D. *et al.* Global and regional estimates of COPD prevalence: Systematic review and meta-analysis. *J Glob Health* **5**, 020415 (2015).
11. Rivera, R. M., Cosio, M. G., Ghezzi, H., Salazar, M. & Pérez-Padilla, R. Comparison of lung morphology in COPD secondary to cigarette and biomass smoke. *Int. J. Tuberc. Lung Dis.* **12**, 972–977 (2008).
12. Sun, W., Wu, R. & Last, J. A. Effects of exposure to environmental tobacco smoke on a human tracheobronchial epithelial cell line. *Toxicology* **100**, 163–174 (1995).
13. WHO | Burden of COPD. *WHO* <https://www.who.int/respiratory/copd/burden/en/>.
14. Vogelmeier, C. F. *et al.* Global Strategy for the Diagnosis, Management, and Prevention of Chronic Obstructive Lung Disease 2017 Report. GOLD Executive Summary. *Am J Respir Crit Care Med* **195**, 557–582 (2017).
15. Hogg, J. C. Pathophysiology of airflow limitation in chronic obstructive pulmonary disease. *Lancet* **364**, 709–721 (2004).
16. Janoff, A. & Zeligs, J. D. Vascular injury and lysis of basement membrane in vitro by neutral protease of human leukocytes. *Science* **161**, 702–704 (1968).
17. Hunninghake, G. M. *et al.* MMP12, lung function, and COPD in high-risk populations. *N. Engl. J. Med.* **361**, 2599–2608 (2009).
18. Silverman, E. K. & Sandhaus, R. A. Alpha1-Antitrypsin Deficiency. *New England Journal of Medicine* **360**, 2749–2757 (2009).
19. Janciauskiene, S. *et al.* The Multifaceted Effects of Alpha1-Antitrypsin on Neutrophil Functions. *Front. Pharmacol.* **9**, (2018).
20. Shapiro, S. D. *et al.* Neutrophil elastase contributes to cigarette smoke-induced emphysema in mice. *Am. J. Pathol.* **163**, 2329–2335 (2003).
21. Genschmer, K. R. *et al.* Activated PMN Exosomes: Pathogenic Entities Causing Matrix Destruction and Disease in the Lung. *Cell* **176**, 113–126.e15 (2019).
22. Barnes, P. J. Inflammatory endotypes in COPD. *Allergy* **74**, 1249–1256 (2019).
23. Agustí, A. & Hogg, J. C. Update on the Pathogenesis of Chronic Obstructive Pulmonary Disease. *New England Journal of Medicine* **381**, 1248–1256 (2019).
24. Celli, B. R. & Wedzicha, J. A. Update on Clinical Aspects of Chronic Obstructive Pulmonary Disease. *New England Journal of Medicine* **381**, 1257–1266 (2019).
25. Seemungal, T. *et al.* Respiratory viruses, symptoms, and inflammatory markers in acute exacerbations and stable chronic obstructive pulmonary disease. *Am. J. Respir. Crit. Care Med.* **164**, 1618–1623 (2001).
26. Papi, A. *et al.* Infections and airway inflammation in chronic obstructive pulmonary disease severe exacerbations. *Am. J. Respir. Crit. Care Med.* **173**, 1114–1121 (2006).
27. Barnes, P. J. Targeting cytokines to treat asthma and chronic obstructive pulmonary disease. *Nature Reviews Immunology* **18**, 454–466 (2018).
28. Givi, M. E., Redegeld, F. A. & Mortaz, G. F. and E. Dendritic Cells in Pathogenesis of COPD. *Current Pharmaceutical Design* vol. 18 2329–2335 <http://www.eurekaselect.com/96642/article> (2012).
29. IARC Working Group on the Evaluation of Carcinogenic Risk to. *Tobacco Smoke and Involuntary Smoking*. (International Agency for Research on Cancer, 2004).

30. Houghton, A. M. *et al.* Elastin fragments drive disease progression in a murine model of emphysema. *J. Clin. Invest.* **116**, 753–759 (2006).
31. Cosio, M. G., Saetta, M. & Agusti, A. Immunologic Aspects of Chronic Obstructive Pulmonary Disease. *New England Journal of Medicine* **360**, 2445–2454 (2009).
32. Saetta, M. *et al.* CD8+ T-Lymphocytes in Peripheral Airways of Smokers with Chronic Obstructive Pulmonary Disease. *Am J Respir Crit Care Med* **157**, 822–826 (1998).
33. Saetta, M. *et al.* CD8 + ve Cells in the Lungs of Smokers with Chronic Obstructive Pulmonary Disease. *Am J Respir Crit Care Med* **160**, 711–717 (1999).
34. Jiang, D., Liang, J., Li, Y. & Noble, P. W. The role of Toll-like receptors in non-infectious lung injury. *Cell Res.* **16**, 693–701 (2006).
35. Parker, L. C., Prince, L. R. & Sabroe, I. Translational Mini-Review Series on Toll-like Receptors: Networks regulated by Toll-like receptors mediate innate and adaptive immunity. *Clin Exp Immunol* **147**, 199–207 (2007).
36. Huang, X. *et al.* Differential DAMP release was observed in the sputum of COPD, asthma and asthma-COPD overlap (ACO) patients. *Scientific Reports* **9**, 1–9 (2019).
37. Noguera, A. *et al.* An investigation of the resolution of inflammation (catabasis) in COPD. *Respir Res* **13**, 101 (2012).
38. Welte, T. & Köhnlein, T. Global and local epidemiology of community-acquired pneumonia: the experience of the CAPNETZ Network. *Semin Respir Crit Care Med* **30**, 127–135 (2009).
39. Ghorani, V., Boskabady, M. H., Khazdair, M. R. & Kianmehr, M. Experimental animal models for COPD: a methodological review. *Tob Induc Dis* **15**, (2017).
40. Beckett, E. L. *et al.* A new short-term mouse model of chronic obstructive pulmonary disease identifies a role for mast cell tryptase in pathogenesis. *J. Allergy Clin. Immunol.* **131**, 752–762 (2013).
41. Sajjan, U. *et al.* Elastase- and LPS-exposed mice display altered responses to rhinovirus infection. *Am J Physiol Lung Cell Mol Physiol* **297**, L931–L944 (2009).
42. Mahadeva, R. & Shapiro, S. D. Chronic obstructive pulmonary disease \* 3: Experimental animal models of pulmonary emphysema. *Thorax* **57**, 908–914 (2002).
43. Lucey, E. C., Keane, J., Kuang, P.-P., Snider, G. L. & Goldstein, R. H. Severity of Elastase-Induced Emphysema Is Decreased in Tumor Necrosis Factor- $\alpha$  and Interleukin-1 $\beta$  Receptor-Deficient Mice. *Laboratory Investigation* **82**, 79–85 (2002).
44. Thiesse, J. *et al.* Lung structure phenotype variation in inbred mouse strains revealed through in vivo micro-CT imaging. *J Appl Physiol* (1985) **109**, 1960–1968 (2010).
45. Weibel, E. R. Principles and Methods of Morphometry. in *Morphometry of the Human Lung* (ed. Weibel, E. R.) 9–39 (Springer, 1963). doi:10.1007/978-3-642-87553-3\_3.
46. Meyerholz, D. K., Suarez, C. J., Dintzis, S. M. & Frevert, C. W. 9 - Respiratory System. in *Comparative Anatomy and Histology (Second Edition)* (eds. Treuting, P. M., Dintzis, S. M. & Montine, K. S.) 147–162 (Academic Press, 2018). doi:10.1016/B978-0-12-802900-8.00009-9.
47. Ochs, M. *et al.* The Number of Alveoli in the Human Lung. *Am J Respir Crit Care Med* **169**, 120–124 (2004).
48. Moon, T. C. *et al.* Advances in mast cell biology: new understanding of heterogeneity and function. *Mucosal Immunology* **3**, 111–128 (2010).
49. Wong, G. W. *et al.* Ancient origin of mast cells. *Biochem. Biophys. Res. Commun.* **451**, 314–318 (2014).
50. da Silva, E. Z. M., Jamur, M. C. & Oliver, C. Mast cell function: a new vision of an old cell. *J. Histochem. Cytochem.* **62**, 698–738 (2014).
51. Plum, T. *et al.* Human Mast Cell Proteome Reveals Unique Lineage, Putative Functions, and Structural Basis for Cell Ablation. *Immunity* **52**, 404–416.e5 (2020).
52. Méndez-Enríquez, E. & Hallgren, J. Mast Cells and Their Progenitors in Allergic Asthma. *Front. Immunol.* **10**, (2019).
53. Li, Z. *et al.* Adult Connective Tissue-Resident Mast Cells Originate from Late Erythro-Myeloid Progenitors. *Immunity* **49**, 640–653.e5 (2018).
54. Elieh Ali Komi, D., Wöhr, S. & Bielory, L. Mast Cell Biology at Molecular Level: a Comprehensive Review. *Clinic Rev Allerg Immunol* (2019) doi:10.1007/s12016-019-08769-2.
55. PGH Gell; RRA Coombs. The classification of allergic reactions underlying disease. *Oxford, Blackwell* 317–227 (1963).
56. Wernersson, S. & Pejler, G. Mast cell secretory granules: armed for battle. *Nat. Rev. Immunol.* **14**, 478–494 (2014).
57. Sibilano, R., Frossi, B. & Pucillo, C. E. Mast cell activation: A complex interplay of positive and negative signaling pathways. *European Journal of Immunology* **44**, 2558–2566 (2014).
58. Xiang, Z., Block, M., Löfman, C. & Nilsson, G. IgE-mediated mast cell degranulation and recovery monitored by time-lapse photography. *J. Allergy Clin. Immunol.* **108**, 116–121 (2001).
59. Mukai, K., Tsai, M., Saito, H. & Galli, S. J. Mast cells as sources of cytokines, chemokines, and growth factors. *Immunol. Rev.* **282**, 121–150 (2018).



60. Galli, S. J. *et al.* Chapter 2 - Approaches for Analyzing the Roles of Mast Cells and Their Proteases In Vivo. in *Advances in Immunology* (ed. Alt, F. W.) vol. 126 45–127 (Academic Press, 2015).
61. Douaiher, J. *et al.* Development of Mast Cells and Importance of Their Tryptase and Chymase Serine Proteases in Inflammation and Wound Healing. *Adv Immunol* **122**, 211–252 (2014).
62. Oskeritzian, C. A. Mast cell plasticity and sphingosine-1-phosphate in immunity, inflammation and cancer. *Mol. Immunol.* **63**, 104–112 (2015).
63. Rabelo Melo, F., Santosh Martin, S., Sommerhoff, C. P. & Pejler, G. Exosome-mediated uptake of mast cell tryptase into the nucleus of melanoma cells: a novel axis for regulating tumor cell proliferation and gene expression. *Cell Death & Disease* **10**, 1–16 (2019).
64. Russi, A. E., Walker-Caulfield, M. E. & Brown, M. A. Mast cell inflammasome activity in the meninges regulates EAE disease severity. *Clin. Immunol.* **189**, 14–22 (2018).
65. Krystel-Whittemore, M., Dileepan, K. N. & Wood, J. G. Mast Cell: A Multi-Functional Master Cell. *Front Immunol* **6**, 620 (2015).
66. Möllerherm, H., von Köckritz-Blickwede, M. & Branitzki-Heinemann, K. Antimicrobial Activity of Mast Cells: Role and Relevance of Extracellular DNA Traps. *Front Immunol* **7**, (2016).
67. Virk, H., Arthur, G. & Bradding, P. Mast cells and their activation in lung disease. *Translational Research* **174**, 60–76 (2016).
68. Varricchi, G. *et al.* Heterogeneity of Human Mast Cells With Respect to MRGPRX2 Receptor Expression and Function. *Front. Cell. Neurosci.* **13**, (2019).
69. Salomonsson, M. *et al.* Circulating mast cell progenitors correlate with reduced lung function in allergic asthma. *Clin. Exp. Allergy* **49**, 874–882 (2019).
70. Komi, D. E. A. *et al.* The Role of Mast Cells in IgE-Independent Lung Diseases. *Clinic Rev Allerg Immunol* **58**, 377–387 (2020).
71. Collington, S. J., Williams, T. J. & Weller, C. L. Mechanisms underlying the localisation of mast cells in tissues. *Trends Immunol.* **32**, 478–485 (2011).
72. Shin, K. *et al.* Mouse Mast Cell Tryptase mMCP-6 Is a Critical Link between Adaptive and Innate Immunity in the Chronic Phase of *Trichinella spiralis* Infection. *J Immunol* **180**, 4885–4891 (2008).
73. Feyerabend, T. B. *et al.* Cre-Mediated Cell Ablation Contests Mast Cell Contribution in Models of Antibody- and T Cell-Mediated Autoimmunity. *Immunity* **35**, 832–844 (2011).
74. Shibata, S. *et al.* Basophils trigger emphysema development in a murine model of COPD through IL-4-mediated generation of MMP-12-producing macrophages. *Proc. Natl. Acad. Sci. U.S.A.* **115**, 13057–13062 (2018).
75. Barnes, P. J. Sex Differences in Chronic Obstructive Pulmonary Disease Mechanisms. *Am J Respir Crit Care Med* **193**, 813–814 (2016).
76. Gan, W. Q., Man, S. F. P., Postma, D. S., Camp, P. & Sin, D. D. Female smokers beyond the perimenopausal period are at increased risk of chronic obstructive pulmonary disease: a systematic review and meta-analysis. *Respir. Res.* **7**, 52 (2006).
77. Wilhelmson, A. S. *et al.* Testosterone is an endogenous regulator of BAFF and splenic B cell number. *Nature Communications* **9**, 2067 (2018).
78. Natri, H., Garcia, A. R., Buetow, K. H., Trumble, B. C. & Wilson, M. A. The Pregnancy Pickle: Evolved Immune Compensation Due to Pregnancy Underlies Sex Differences in Human Diseases. *Trends in Genetics* **35**, 478–488 (2019).
79. Kim, T.-S. & Shin, E.-C. The activation of bystander CD8 + T cells and their roles in viral infection. *Experimental & Molecular Medicine* **51**, 1–9 (2019).
80. Raué, H.-P., Brien, J. D., Hammarlund, E. & Slifka, M. K. Activation of Virus-Specific CD8+ T Cells by Lipopolysaccharide-Induced IL-12 and IL-18. *The Journal of Immunology* **173**, 6873–6881 (2004).
81. Parham, P. *The Immune System*. (Garland Science, 2015).